POWER QUALITY MEASUREMENT SYSTEM BASED ON A DIGITAL SIGNAL PROCESSOR

Aleksandar Prodic and Predrag Pejovic*

EPS-JP Elektrovojvodina, ED "Novi Sad" - Novi Sad
Bul. Oslobodjenja 100, 21 000 Novi Sad, Yugoslavia
Tel:+381 21 21 426 - Fax: +381 21 21 426 - E-mail: Aleksandar.Prodic@ns.ev.co.yu

***Faculty of Electrical Engineering, University of Belgrade**
Bul. Revolucije 73, 11 000 Beograd, Yugoslavia
Tel:+381 11 321 8313 - E-mail:peja@el.etf.bg.ac.yu

INTRODUCTION

Rapidly growing number of nonlinear loads increased harmonic pollution in the electric utility systems. Problems related with the harmonic pollution, such as overheating, reduced reliability, and malfunction of electric equipment, as well as interference problems common to sensitive electronic equipment and computers, increased concern about the power quality phenomena. In this paper a system intended for measurement of the power quality parameters is described.

SYSTEM DESCRIPTION

The system is based on a digital signal processor, and it could be used for measurements of power, apparent power, power factor, total harmonic distortion, total demand distortion, as well as spectral analysis of voltages and currents in three phase systems. Long time recordings and event triggering and handling are provided using a connection to a PC laptop computer via RS-232 serial bus. In this manner a simple, cheap and reliable multifunctional power quality measurement system is obtained. Various algorithms applied to process data samples and to compute the power quality parameters are described and tested. Range of the measurement error is discussed.

HARDWARE

Structure of the power quality measurement system is presented in Fig. 1. The system consists of current and voltage transducers, six-channel analog to digital converter, digital signal processor and a communication port applied to provide data exchange with the personal computer. Digital signal processor ADSP-2181 is applied.

Instantaneous values of the currents for all three of the phases are measured applying current clamps or current transformers. The system measurement range depends on the transducing ratio of the current sensing devices. Voltages up to 500 Vrms can be directly connected to the voltage inputs, which are achieved by voltage sensors that provide electric insulation and downscaling of the voltages. Accuracy of these sensoring devices significantly affects accuracy of the measurement system.

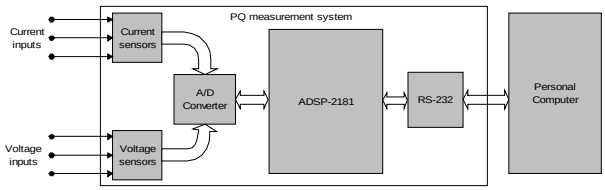

Fig. 1. Block diagram of the power quality measurement system.

The six-channel analog to digital converter (ADC) provides asynchronous sampling and communication with the digital signal processor via duplex serial communication. The ADC operating mode is controlled by the processor which selects sampling rate, input range, output data format and determines which of the analog inputs is active. Resolution of the ADC is 16 bits. Sampling rate can be chosen from a discrete set of fourteen frequencies.

Programmable digital signal processor (DSP) ADSP-2181 is applied to process the data provided by the ADC. It is a single-chip 16-bit microcomputer optimized for digital signal processing [1]. The DSP integrates 80K bytes on chip memory configured in 16K 24-bit words of program memory, and 16K of 16-bit words (16-bit) of data memory. Architecture of the processor enables very fast signal processing and real-time data analysis in the power quality measurement system. The DSP incorporates two complete synchronous serial ports. One of them is reserved for communication with the analog to digital converter, while the other one is used for communication with the personal computer.

Personal computer equipped by a specially developed software, described in this paper, performs acquisition, storage, and additional processing of the measurement results, such as flicker measurement, long time recordings of the power quality parameters, event triggering and handling.

SPECTRAL ANALYSIS

To analyze spectral properties of measured voltages and currents, the discrete Fourier transform (DFT) defined as

$$X[k] = X\left(\frac{2k\pi}{\mathrm{N}}\right) = \sum_{n=0}^{N-1} x[n] e^{-\mathrm{j}\frac{2\pi kn}{N}} \qquad (1)$$

where $k = 0, 1, 2, \ldots N-1$ is applied. In (1) *x[n]* represent discrete time samples of a signal *x(t)*, i.e. *x[n]=x(*nT), where *T* is the time interval between two consequent samples, and *NT* is the signal observation period, which should be equal to a multiple of the signal period.

To improve computational efficiency, DFT defined by (1) is computed applying the fast Fourier transform (FFT) algorithm [2]. In the signal processor radix-2 decimation in time algorithm [3] is implemented.

The sampling system provides asynchronous sampling. Synchronous sampling, which will require synchronizing with the line frequency by a phase locked loop is avoided as an expensive and non-standard solution. Asynchronous sampling result in non-exact matching of the observation interval and line period, in turn resulting in spectral leakage. In Fig. 2 FFT results of a 50 Hz sine wave signal are presented. In the left diagram of Fig. 2 period of the signal and observation period are exactly matched, while in the diagram on the right hand side results obtained with the frequency mismatch of 2 Hz are presented. Spectral leakage effects could be readily observed.

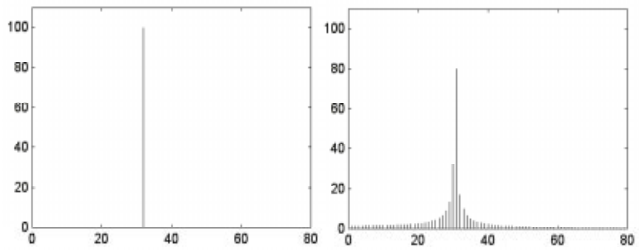

Fig. 2. Illustration of the spectral leakage effects.

Spectral leakage effects can be reduced applying special weight functions, known as window functions [4]. There is a variety of window functions. Good selection of the window function should provide good attenuation at higher frequencies and precise separation of narrow spectral components. These requirements are in frequency domain described by a narrow main-lobe and low amplitudes of high order lobes. Requirements for a window function with extremely narrow main-lobe and very low amplitudes of high order lobes oppose each other. Designer has to make a compromise, and to select suitable window function for specific application.

Choice of the window function for this application is a compromise between accuracy and the measurement range [5]. The Rife-Vincent window functions [6] are chosen, since they are suitable for achieving mentioned task with selection one of there classes. Class I of these functions provides the minimum high order side-lobes' amplitudes, while the class II provides the minimum main-lobe width.

Implementation of the class I Rife-Vincent function exposed high accuracy in determination of the harmonic component amplitudes. For any kind of distorted signal accuracy better than one per cent can be achieved. For the network frequency of 50 Hz measurement range is limited up to 15-th harmonic. This limitation arises from the wide main-lobe.

Selected window function has the first side lobe with minimal attenuation of 80 dB, and it starts at discrete frequency of $\pi/8$. This means that for frequency change Δf of 50 Hz (distance between line frequency harmonics) maximal sampling frequency f_s should not exceed value defined by equation $\pi/8=2\pi\Delta f/f_s$. In this case maximal sampling frequency is 1,5 kHz. Maximal input signal frequency that can be analyzed with applied sampling rate is 750 Hz (fifteenth harmonic frequency).

Simulation results achieved by the implementation of the FFT algorithm and Rife-Vincent class I fourth order [6] window function of the signal with equal amplitudes of the first three harmonic components are presented in Fig. 3. The result is compared to the case when windowing is not applied.

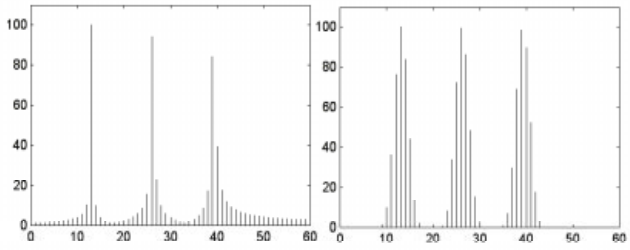

Fig. 3. Spectra of the signal computed without (left), and with windowing (right)

Fig. 3 shows that applied window function provides good separation of frequency components. All samples are divided in three groups, each of the group representing one of the signal components. Application of the interpolation functions [7] enables accurate calculation of frequency and amplitude of each spectral component.

Class II of Rife-Vincent functions provides narrow main lobe, but it has lower attenuation of higher harmonic components. With the use of the same order class II Rife-Vincent window function the range can be tripled. In this case, accuracy can not be exactly defined, and it is dependent by the form of the analyzed signal.

MEASUREMENT OF THE LINE FREQUENCY

Information about the line frequency is very important in a computation of a number of power quality parameters. In the presented system the line frequency is being measured applying programmable timer integrated in the digital signal processor.

For low frequency measurements, the best approach is measurement of the time interval between two moments, when the observed signal reaches defined constant value from the same directions (previous signal values should be higher or lower in the both moments) [8].

The programmable timer defines unity time interval, denoted by T_{TIMER}. The line period T is determined by NT_{TIMER}, where N is a number of timer intervals that passes during one period of the measured signal. The frequency is determined as $1/NT_{TIMER}$. Accuracy of the measurement is determined by T/T_{TIMER} ratio.

Selection of good period boundary values is very important for precise measurement, especially if the signal contains high frequency noise. Counting starts and stops when input signal reaches zero. Noise could cause fault in determination of the stopping moment and thus error in the measurement. To reduce that, stopping of counter is disabled during the first fifty timer periods. It significantly reduces the noise influence. In this case, frequency of the measured signal is $1/(2NT_{TIMER})$, and maximal error of the measurement is determined as $\Delta T = 2\ T_{TIMER}$.

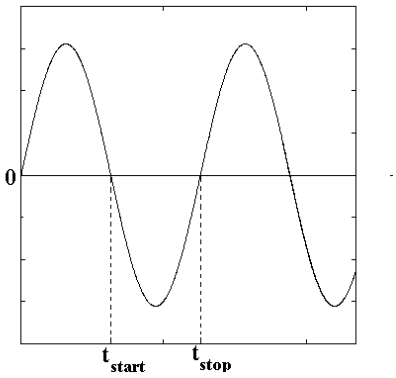

Fig.4. Observation period for frequency measurement

Low T_{TIMER} value enables accurate measurement. Noise, sudden voltage variations and presence of dc component are dominant causes of the measurement error. Mentioned effects are not predictable, and to reduce their effects the device calculates frequency values in twenty five periods and computes average value.

MEASUREMENT OF RMS VALUES

Measurement of the voltage and current rms values is obtained by processing samples of the measured signals. Sampled signal rms value is defined as

$$X_{RMS} = \sqrt{\frac{1}{N}\sum_{n=1}^{N}(x[n])^2} \qquad (2)$$

where $x[n]$ presents samples of the signal whose rms value is being calculated, and N is the number of samples per line period. This algorithm is computationally efficient and it is applied in other computations, for example in the apparent power, THD, and TDD measurements.

Choice of the number of samples for computation of the rms values

The number of points N, applied to compute the rms values is extremely important for accuracy of the measurement. To obtain correct results for the rms values N/f_{sample} should be equal to a multiple of the line period. To determine number of points, previously measured frequency and applied sampling frequency (f_{sample}) are considered, and the number of points is determined as

$$N = L\frac{f_{sample}}{f} \qquad (3)$$

where L is an integer. Choosing large values for the parameter L averaging of the rms value can be provided. It also provides more accurate calculation of rms values. Error of the measurement linearly decreases with the increase of number of points N.

MEASUREMENTS OF POWER

The system provides measurement of average and apparent power by processing of the sampled current and voltage signals. Measurement of the power factor is based on the average and apparent power measurements.

Average power P is computed as

$$P = \frac{1}{N}\sum_{n=1}^{N} v[n]\,i[n] \qquad (4)$$

The number of samples N is chosen according to (3) to provide averaging.

The apparent power is computed as

$$S = V_{RMS}\ I_{RMS} \qquad (5)$$

where V_{RMS} and I_{RMS} are rms values of a corresponding voltage and current, computed as defined by (2).

Finally, the power factor is computed as

$$PF = \frac{P}{S} \tag{6}$$

MEASUREMENT OF THE TOTAL HARMONIC DISTORTION

Total harmonic distortion (THD) is a quantitative measure of a signal distortion, defined as

$$THD_X = \frac{100\%}{X_{1RMS}} \sqrt{\sum_{n=2}^{\infty} X_{nRMS}^2} \tag{7}$$

where X_{nRMS} is rms value of the signal n-th harmonic component.

The first harmonic extraction

Extraction of the first harmonic by multiplication of the input samples with $sin[\omega_1 n]$ and $cos[\omega_1 n]$ values (ω_1 is a discrete frequency presentation of the first harmonic frequency), additional extraction of dc components (X_{1S} and $X_{1c,}$ respectively) from obtained results and calculation of the first harmonic X_1 as

$$X_1 = \sqrt{X_{1C}^2 + X_{1S}^2} \tag{8}$$

demands calculation of weighting sin/cos values for each sample. Frequency variation disables use of look up tables with constant values. This process is time-consuming.

To improve computation efficiency discrete filtering is applied. Line frequency of 50 Hz determinates filter's characteristics, and it is designed as a low-pass filter with 55 Hz pass-band boundary and 90 Hz cut-off frequencies. For accurate measurement, filter is required to have low amplitude variations (less then one per cent) in pass-band area and high attenuation of higher frequencies (greater then 40 dB at cut-off frequency).

Considering characteristics at the pass-band boundary, transition and stop-band areas, The Chebyshev filter is chosen. The seventh order, the first class Chebyshev filter satisfies mentioned demands for accuracy. Amplitude characteristics of filter are given on Fig. 5.

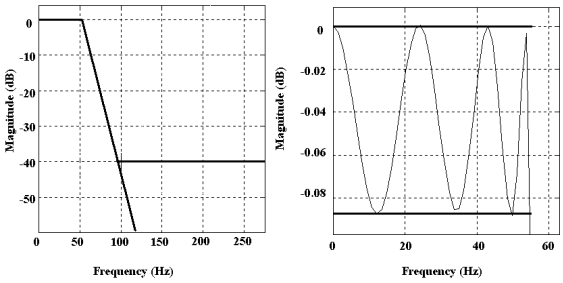

Fig. 5. Amplitude characteristics of the first harmonic filter

Pass-band characteristic (Fig. 5, on the right hand side) shows that less then 1% amplitude variation in the whole area is achieved. Stop-band characteristics shows that attenuation of 40 dB for 50 Hz frequency difference is achieved, so the less then 1% of second harmonic is added on the first harmonic value. It also shows that impact of higher harmonics can be neglect.

Amplitude characteristics of high order filters are very sensitive on effects caused by coefficientes quantization [9], inevitable with fix-point arithmetic that processor performs, especially if the direct form of infinite impulse response filter is implemented. Less sensitive amplitude characteristics with good disposition of poles is achieved by use of cascade connection of modified second-order biquad sections [9]. The second-order modified biquad section is presented in Fig. 6.

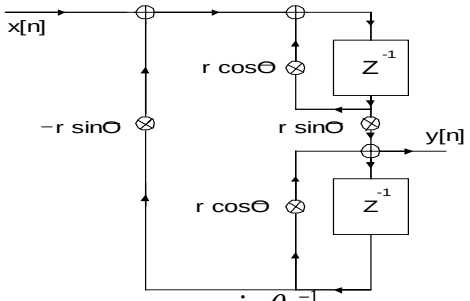

$$H(z) = \frac{r \sin\theta z^{-1}}{1 - (2r\cos\theta) z^{-1} + r^2 z^{-2}} \tag{9}$$

Fig. 6. Second-order modified biquad section

A par of complex poles is presented as

where the par of complex poles is represented by $re^{-/+j\theta}$.

The fixed point presentation allowes finite number of values for the coefficientes presentation, thus the difference between calculated and implemented values of filter coefficientes exists. Better disposition of poles reduces this mismatching, it is achieved by implementation of biquad section presented in Fig. 6. and in (9).
When rms value of the first harmonic is calculated, the THD value is computed applying

$$THD_X = \frac{100\%}{X_{1RMS}} \sqrt{X_{RMS}^2 - X_{1RMS}^2} \,. \qquad (10)$$

Total demand distortion (TDD) is defined in a similar way, and the only difference from the definition (7) is in the denominator, which is in this case the value that characterizes the consumer (rated rms value of the voltage, maximal rms value of the current, defined by permission given from the electric utility company, etc.).

VOLTAGE FLUCTUATIONS (FLICKER) MEASUREMENT

Voltage fluctuations are systematic variations of the voltage envelope or a series of random voltage changes, the magnitude of which does not normally exceed the voltage ranges specified by the other power quality parameter limits. These variations are referred as flicker [10].

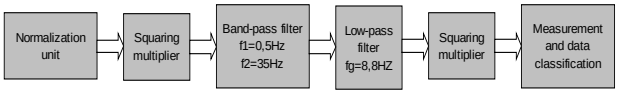

Fig. 7. Functional diagram of IEC flickermeter

Originally, flicker is impact of these voltage fluctuations on lamps that can be sensed by human eyes. Impact of the flicker is determined by the amplitude and frequency fluctations of the supply voltage. Previously, this impact was calculated by the measurement of the voltage changes and by their comparison with flicker sensitivity curves. In the IEC standards a rigorous approach is applied, and specifications for the flicker measurement are given by IEC-868. Simplified functional diagram of IEC flickermeter is given in Fig. 7.

The system presented in Fig. 7 simulates human eyes and brain sensitivity on changes caused by the variations of the artificial light. Blocks for normalization and squaring simulate behavior of the lamp. Band-pass filter eliminates the dc component and removes spectral components at frequency higher than 35 Hz, simulating behavior of human eyes. Narrow band-pass filter with central frequency of 8.8 Hz and another squaring block simulate response of a human brain. Finally, the results are measured and classified according to the rules given by IEC-868.

Dynamics of the flicker is in the low frequency area, thus its computation and acquisition of the results can be performed by a personal computer. The digital signal processor based system in this case is applied only for voltage measurement and data transfer.

ERRORS OF THE MEASUREMENTS

Sources of the measurement error could be classified in four groups: errors caused by finite accuracy of the analog transducers, errors caused by the analog to digital conversion, errors caused by finite digital word length, and errors caused by the digital signal processing methods.

Physical characteristics and construction of the transducers determinate their accuracy. Current transformers that are used for switchgear metering and relaying have accuracy better then 3% in the frequency range up to 10 kHz. If the current transformer burden is inductive, a phase shift in the measured current could be expected. To avoid the phase shift errors, Hall-effect transducers or compensated current clamps should be used.
Voltages up to 500 V rms can be directly connected on the voltage inputs of the proposed system. Accuracy of the voltage sensors is ±0.6% at 25°C. For measurements at higher voltages additional voltage transducers or voltage dividers have to be applied. Magnetic voltage transducers, available in the most of the plants are designed to operate at the line frequency. For harmonic components of frequency less than 5 kHz the accuracy is usually within 3%, which is satisfactory according to the IEEE Standard 519-1992 [11].

Finite duration of the analog to digital conversion process and finite length of the digital word introduce error in the conversion process. In comparison to the measured signal dynamics, the conversion process is much faster, thus the error caused by the finite duration of the conversion process can be neglected. Analog signals are after the conversion represented by 16-bit digital words, causing quantization error. Error introduced by the analog to digital conversion process can be significantly reduced by selectable conversion range, supported by applied analog to digital converter.

CONCLUSIONS

A system for three-phase, real-time measurement of power quality parameters is presented. Algorithms for different measurements are presented and illustrated by simulation results. It is shown that problems related to spectral leakage caused by asynchronous sampling can be reduced applying window functions. Compromise between accuracy and the measurement range in spectral analysis is achieved by the selection of appropriate window function. A method for accurate frequency measurement is given. Measurement error is studied in detail.

REFERENCES

[1] ADSP-2100 Family User's Manual, Analog Devices, Inc., pp.1.1-1.11., September 1995.

[2] Proakis, J.G., and Manolakis, Introduction to Digital Signal Processing, Macmillan Publishing Company, New York, 1988.

[3] Digital Signal Processing Applications Using the ADSP-2100 Family, Analog Devices, Inc., pp.181-193, 1992.

[4] F. J. Harris, On the Use of Windows for Harmonic Analysis with Discrete Fourier Transform, IEEE, vol. 66, No. 1, pp. 51-83, January 1978.

[5]G. Andria, M. Savino, Windows and Interpolation Algorithms to Improve Electrical Measurement Accuracy, IEEE Transactions on Instrumentation and Measurement, vol. 38., No. 4, pp. 856-863, August 1989.

[6] D. C. Rife and G. A. Vincent, Use of the Discrete Fourier Transform in the Measurement of Frequencies and Levels of Tones, The Bell System Technical Journal, pp.197-228, February 1970.

[7] V. K. Jain, W. L. Collins, D.C. Davis, High-Accuracy Analog Measurements via Interpolated FFT, IEEE Transaction on Instrumentation and Measurement.

[8] J. B. Peatman, Design with Microcontrollers, McGraw-Hill international editions, pp.65-75, September 1988.

[9] Avenhaus, E. and Schussler, W., "On the Approximation Problem in the Design of Digital Filters with Limited Wordlength", Arch. Elektronik Ubertragung., Vol.24, pp.571-572, 1970.

[10] The Voltech Handbook of Testing to IEC-555, Voltech Application note 104, pp. 13-25 and 53-59, November 1994.

[11] IEEE-519, IEEE Recommended Practices and Requirements, 1992.